Self-stabilization of high-frequency oscillations in semiconductor superlattices by time-delay autosynchronization

J. Schlesner,[1] A. Amann,[1] N. B. Janson,[1,2] W. Just,[1,3,*] and E. Schöll[1]
[1]*Institut für Theoretische Physik, Technische Universität Berlin, Hardenbergstraße 36, D-10623 Berlin, Germany*
[2]*Department of Physics, Lancaster University, Lancaster LA1 4YB, United Kingdom*
[3]*Theoretische Physik I, Technische Universität Chemnitz, D-09107 Chemnitz, Germany*
(Received 21 March 2003; revised manuscript received 17 September 2003; published 24 December 2003; publisher error corrected 26 January 2004)

We present a scheme to stabilize high-frequency domain oscillations in semiconductor superlattices by a time-delayed feedback loop. Applying concepts from chaos control theory we propose to control the spatiotemporal dynamics of fronts of accumulation and depletion layers which are generated at the emitter and may collide and annihilate during their transit, and thereby suppress chaos. The proposed method only requires the feedback of internal global electrical variables, viz., current and voltage, which makes the practical implementation very easy.

DOI: 10.1103/PhysRevE.68.066208 PACS number(s): 05.45.Gg, 05.45.Pq, 72.20.Ht, 73.61.−r

Semiconductor superlattices [1] have been demonstrated to give rise to self-sustained current oscillations ranging from several hundred megahertz [2–4] to 150 GHz at room temperature [5], which promises potentially important applications as electronic oscillators. Various mechanisms with [6–9] or without [10] the involvement of propagating field domains have been discussssed. In any case, a superlattice constitutes a highly nonlinear system [11], and instabilities are likely to occur. Indeed, chaotic scenarios have been found experimentally [12–14] and described theoretically in periodically driven [15] as well as in undriven systems [16]. For a reliable operation of a superlattice as an ultrahigh-frequency oscillator such unpredictable and irregular conditions should be avoided. In principle, synchronization of oscillations in a superlattice by an external signal [2,17] could be exploited to achieve a desired periodic behavior. However, in reality, the control of the forcing frequency in the ultrahigh range presents substantial technical problems.

Here, we propose a simple self-stabilizing scheme that is especially suitable for semiconductor devices such as superlattices. It uses a profound concept of chaos control from nonlinear dynamics and chaos theory. Within this approach, an intrinsically unstable time-periodic motion is stabilized using a simple feedback loop, which couples back the difference of an output variable at the actual time t and the same variable at a delayed time $t-\tau$ [18]. This type of control needs only small control forces initially, and they vanish once control has been achieved. A sound advantage is that the oscillation mode to be stabilized need not be known beforehand, in contrast to other chaos control schemes. Rather, a simple delay line in combination with a difference amplifier leads to autosynchronization of the system. Methods of nonlinear control theory [19,20] have been usefully applied to real world problems in various areas of physics, chemistry, and biology [21–29], but no use has been made of this in the field of semiconductor self-oscillators.

Control methods can be either local or global [30]. Local methods require our ability to measure, and apply forcing directly to, the spatially resolved state variables of the system under study. However, in nanotechnology such variables, being, e.g., electron densities in some quantum wells, are not easily accessible, and thus local methods cannot be applied. Unlike those, global methods require access only to some macroscopic variable(s) characterizing some integral output of the system. Such output can generally be reliably measured, and thus global methods seem to be the only option for the control of devices such as superlattices. However, as we will show below, they are not straightforwardly applicable to nanosystems whose structure is spatially discrete. In this paper we present a general approach to self-stabilization of irregular oscillations in semiconductor devices based upon essentially discrete quantum structures.

We consider a model for nonlinear electronic transport in semiconductor superlattices that yields complex and chaotic dynamic behavior under fixed time-independent external voltage in a regime where self-sustained dipole waves [31] are spontaneously generated at the emitter. Those dipole waves are associated with traveling field domains, and consist of electron accumulation and depletion fronts that, in general, travel at different velocities and may merge and annihilate. Such moving fronts are widespread in nonlinear, spatially extended systems, and similar chaotic front patterns occur in many other systems, e.g., spatially continuous models describing bulk impurity impact ionization breakdown in semiconductors [32] or globally coupled heterogeneous catalytic reactions [33]. Thus the time-delay autosynchronization method proposed in this work could be readily applied to stabilize similar space-time patterns in a variety of systems.

Our model of a superlattice is based on sequential tunneling of electrons [31]. In the framework of this model the quantum wells are assumed to be only weakly coupled, and electrons are localized at these wells. Although this approximation is based upon a small miniband width, the resulting transport characteristics have a much wider range of applicability in the high-temperature or the high-field regime (where current oscillations occur) even for strongly coupled quantum wells, as has been demonstrated by a detailed com-

*Permanent address: School of Mathematical Sciences, Queen Mary/University of London, Mile End Road, London E1 4NS, U.K.

parison of the velocity-field characteristics with a full quantum transport model [31]. In Ref. [17] our model was successfully applied to reproduce the observed high-frequency oscillations in a strongly coupled superlattice. The resulting tunneling current density $J_{m\rightarrow m+1}(F_m, n_m, n_{m+1})$ from well m to well $m+1$ depends only on the electric field F_m between both wells and the electron densities n_m and n_{m+1} in the respective wells (in units of cm^{-2}). A typical dependence of $J_{m\rightarrow m+1}$ on the electric field between two consecutive wells is N shaped and exhibits a pronounced regime of negative differential conductivity.

The total applied voltage U between emitter and collector imposes a global constraint $U=-\Sigma_{m=0}^{N}F_m d$, where d is the superlattice period. This, together with Gauss's law, allows us to calculate the fields $F_m(n_1, \ldots, n_N, U)$ for a given electron density distribution.

The rate of variation of the electron density in well m is governed by the continuity equation

$$e\frac{dn_m}{dt}=J_{m-1\rightarrow m}-J_{m\rightarrow m+1} \quad \text{for} \quad m=1,\ldots,N, \tag{1}$$

where N is the number of wells in the superlattice, and $e<0$ is the electron charge.

At the contacts we choose Ohmic boundary conditions. If the contact conductivity σ is chosen appropriately, electron accumulation and depletion fronts are generated at the emitter [16]. Those fronts form a traveling high-field domain, with leading electron depletion front and trailing accumulation front. This leads to self-generated current oscillations. A fixed voltage U imposes a constraint on the lengths of the high-field domains and thus on the front velocities. If N_a accumulation fronts and N_d depletion fronts are present, the respective front velocities v_a and v_d must obey $v_d/v_a = N_a/N_d$. Since the accumulation and depletion fronts can have different velocities, they may collide in pairs and annihilate. At certain combinations of contact conductivity σ and voltage U, chaotic motion arises, when the annihilation of fronts of opposite polarity occurs at irregular positions within the superlattice [16]. The inset of Fig. 1 shows the plane of σ and U, where regions with distinct regimes are marked by different shading. As a computationally convenient criterion for chaos we have used the rapid decay of the autocorrelation function estimated from $n_{20}(t)$. Chaotic regimes are found at low contact conductivity and low voltages, and at higher contact conductivity and higher voltage. Although chaotic motion occurs only in relatively small portions of the control parameter plane, the chaotic regimes have an intricate structure, and it appears difficult to predict and avoid these in real experiments. For a stable operation even in case of parameter fluctuations it is desirable to suppress these throughout the oscillatory regime. In Fig. 1, a one-parameter bifurcation diagram is given, obtained by plotting the time differences Δt between two consecutive maxima of the electron density in a specified well. Chaotic bands and periodic windows can be clearly seen.

The transition from periodic to chaotic oscillations is enlightened by considering the space-time plot for the evolution of the electron densities [Fig. 2(a)]. At $U=1.15$ V cha-

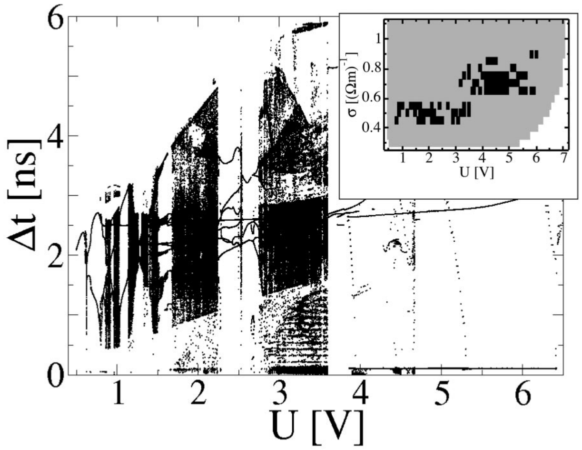

FIG. 1. One-parameter bifurcation diagram: Time differences between consecutive maxima of the electron density in well no. 20 vs voltage U at $\sigma=0.5\ \Omega^{-1}\mathrm{m}^{-1}$. Time series of length 600 ns have been used for each value of the voltage. The inset shows a two-parameter bifurcation diagram: black squares denote chaotic oscillations, light shading indicates periodic oscillations, and the white region shows the absence of oscillations. Simulation of a $N=100$ superlattice with $\mathrm{Al_{0.3}Ga_{0.7}As}$ barriers of width $b=5$ nm and GaAs quantum wells of width $w=8$ nm, doping density $N_D=1.0\times10^{11}\ \mathrm{cm}^{-2}$ and scattering induced broadening $\Gamma=8$ meV at $T=20$ K.

otic front patterns with irregular sequences of annihilation of front pairs at varying positions within the superlattice occur. We have calculated the largest Lyapunov exponent as $1.1\times10^{9}\ \mathrm{s}^{-1}$, which is a clear indication of chaos.

We shall now introduce a feedback loop to control the chaotic front motion and stabilize a periodic oscillation mode which is inherent in the chaotic attractor. Our scope is twofold. We want to suppress the chaotic motion, but in addition the control force should be small, i.e., asymptotically zero, in order to stabilize a proper periodic state of the system. Thus we have to resort to noninvasive control schemes. For the noninvasive stabilization of time-periodic target states a very simple and successful scheme has been proposed [18] using time-delayed signals. An extension of that idea was suggested by Socolar *et al.* [34], using multiple-time delays in order to improve the control performance. Analytical insight into those schemes has been gained only recently [35–37], and various ways of coupling of the control force, including local and global schemes, have been compared [30,38–40]. Whereas local coupling schemes usually lead to efficient control in a large control domain, they are not easily implemented in real systems since local, spatially resolved measurements are necessary. Therefore, here we propose a much simpler global scheme.

In our problem, as a global output signal that is coupled back in the feedback loop, it is natural to use the total current density J defined as follows: $J=\Sigma_{m=0}^{N}J_{m\rightarrow m+1}1/(N+1)$ [31]. For the uncontrolled chaotic oscillations, J is given in Fig. 2(a) by gray, showing irregular spikes at those times when two fronts annihilate. Note that the gray current time trace is modulated by fast small-amplitude oscillations (due

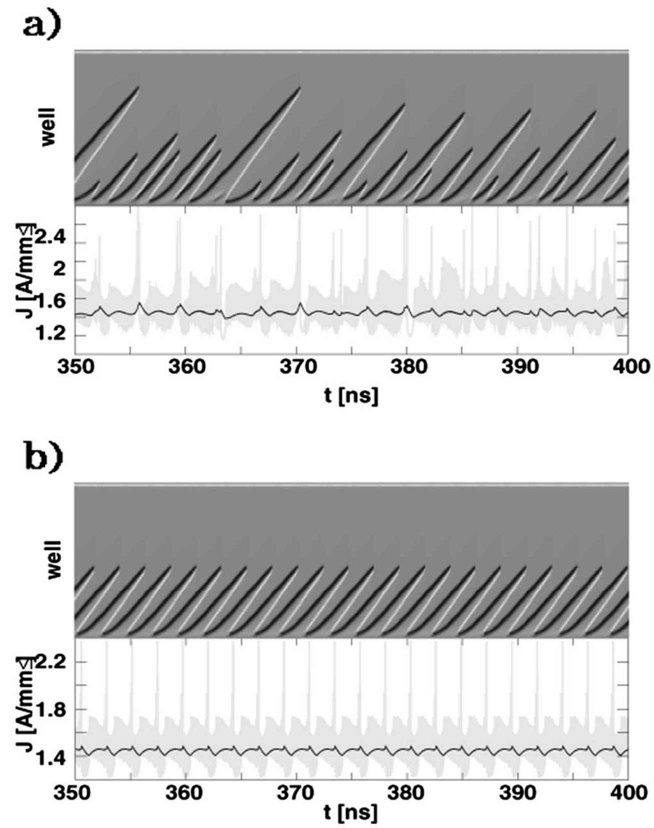

FIG. 2. Control of chaotic front dynamics by extended time-delay autosynchronization. (a) Space-time plot of the uncontrolled charge density, and current density J vs time. (b) Same with global voltage control with exponentially weighted current density (denoted by the black curve). Parameters as in Fig. 1, $U=1.15$ V, $\tau=2.29$ ns, $K=3\times10^{-6}$ V mm^2/A, $R=0.2$, $\alpha=10^9$ s^{-1}. Light and dark regions denote electron accumulation and depletion fronts in the space-time plots of the charge densities, respectively.

to well-to-well hopping of depletion and accumulation fronts in our discrete model), which are not resolved in the plot. However, as the variable J is fed back to the system for the purposes of control, these high-frequency oscillations render the control loop unstable. They need to be filtered out by using, e.g., the following low-pass filter

$$\overline{J}(t)=\alpha\int_0^t J(t')e^{-\alpha(t-t')}\mathrm{d}t', \tag{2}$$

with a cutoff frequency α.

The information contained in the low-frequency part of the current (Fig. 2, black curve) is then used as input in the extended multiple-time autosynchronization scheme. The voltage across the superlattice is modulated by multiple differences of the filtered signal at time t and at delayed times $t-\tau$

$$U=U_0+U_c(t)$$

$$U_c(t)=-K(\overline{J}(t)-\overline{J}(t-\tau))+RU_c(t-\tau)$$

$$=-K\sum_{\nu=0}^{\infty}R^{\nu}(\overline{J}(t-\nu\tau)-\overline{J}[t-(\nu+1)\tau]), \tag{3}$$

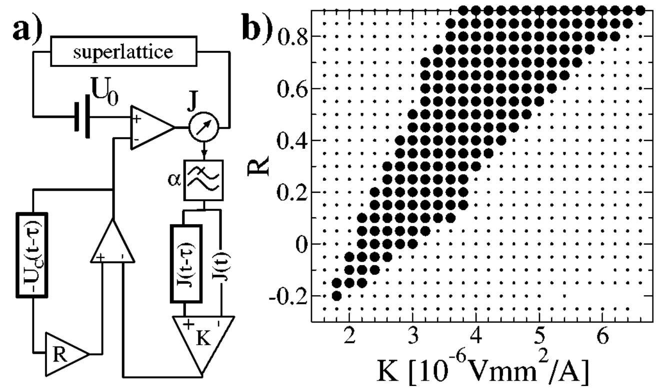

FIG. 3. (a) Control circuit including the low-pass filter with cutoff frequency α and the time-delayed feedback loop (K) and its extension to multiple time delays (R). (b) Control domain for global voltage control. Full circles denote successful control, small dots denote no control. Parameters as in Fig. 2.

where U_0 denotes a time-independent external bias and U_c is the control voltage. The control parameters are given by the amplitude of the control force K and the memory parameter R, whereas the delay time τ is adjusted to the period of the orbit. The period τ, i.e., suitable choices for the delay time, can be determined *a priori* by observing the resonance-like behavior of the mean control force versus τ. A sketch of the whole control circuit is displayed in Fig. 3(a). Such a global control scheme is easy to implement experimentally. It is noninvasive in the sense that the control force vanishes when

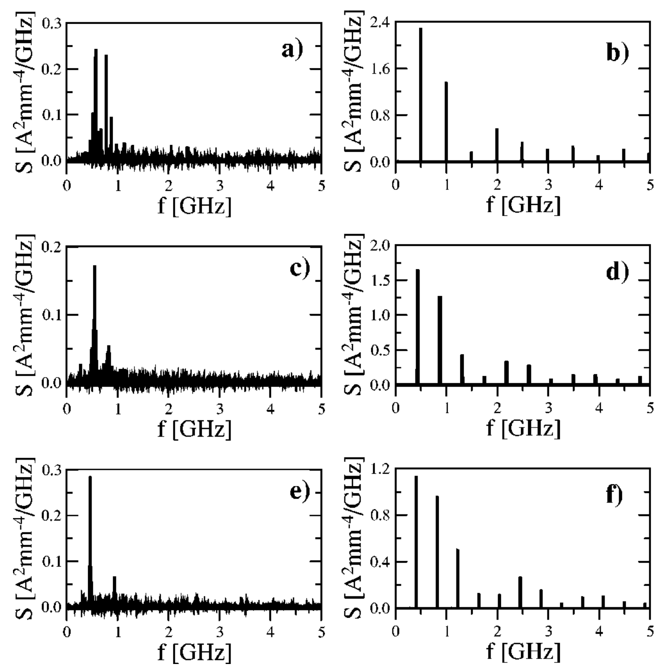

FIG. 4. Fourier power spectra of controlled oscillations as compared to those of uncontrolled ones. For $\sigma=0.5\ \Omega^{-1}$ m^{-1} three values of applied voltage U are taken at which the system demonstrates chaotic oscillations (see Fig. 1): (a),(b) $U=1$ V, $\tau=2.0091$ ns, (c),(d) $U=1.15$ V, $\tau=2.2900$ ns, (e),(f) $U=1.25$ V, $\tau=2.4469$ ns, $R=0.5$. Left column: without control, right column: with control. Other parameters as in Fig. 2.

the target state of period τ has been reached. This target state is an unstable periodic orbit of the uncontrolled system. The result of the control is shown in Fig. 2(b). The front dynamics exhibits annihilation of front pairs at fixed positions within the superlattice, and stable periodic oscillations of the current are obtained.

In Fig. 3(b) the control domain is depicted in the parameter plane of R and K. A typical hornlike control domain similar to those known from other coupling schemes [30] is found. Control is achieved in a range of values of the control amplitude K, which is widened and shifted to larger K with increasing memory parameter R. Typically, the left-hand control boundary corresponds to a period-doubling bifurcation leading to chaos for smaller K, while the right-hand boundary is associated with a Hopf bifurcation. The shape of our control domain and its size resemble the results obtained analytically for diagonal control schemes where observables are measured and controlled locally. In particular we do not observe the influence of other branches of the Floquet eigenvalue problem, which might reduce the size of the control domain severely [41]. Thus our control scheme is of similar control performance as local control.

To illustrate the effect of control on the distribution of oscillation energy over the frequencies, we present Fourier power spectra of the current density J without control, to be compared with those when the control is applied. We fix $\sigma = 0.5\ \Omega^{-1}\ \mathrm{m}^{-1}$ as in Fig. 1, and select three values of U where chaotic oscillations exist. The Fourier spectra of uncontrolled oscillations are given in Figs. 4(a), 4(c), and 4(e) for $U=1$ V, $U=1.15$ V, and $U=1.25$ V, respectively. All three spectra are continuous over frequency, although they contain distinct peaks. The spectra of the controlled oscillations become discrete [Figs. 4(b), 4(d), and 4(f)] thus reflecting their periodicity. The spiky shape of the oscillations results in a large content of harmonics. With respect to the implications of global chaos control for the generation of tunable high-frequency oscillations, it is important to note that the fundamental frequency decreases with increasing voltage U from 0.5 GHz [$U=1$ V, (b)] to 0.4 GHz [$U=1.25$ V, (f)].

To conclude, we have demonstrated that time-delay autosynchronization represents a convenient and simple scheme for the self-stabilization of high-frequency current oscillations due to moving domains in superlattices. This approach lacks the drawback of synchronization by an external ultrahigh-frequency forcing, since it requires nothing but delaying of the global electrical system output by the specified time lag. The proposed low-pass filtering of the output signal presents a solution of the problem one necessarily encounters when trying to control a nanosystem with a crucially discrete quantum structure leading to superimposed fast well-to-well hopping oscillations in our case.

This work was supported by DFG in the framework of Sfb 555 and through Grant No. JU261/3-1. N.J. acknowledges partial support by EPSRC. We gratefully acknowledge discussion with A. Wacker.

[1] L. Esaki and R. Tsu, IBM J. Res. Dev. **14**, 61 (1970).
[2] J.F. Cadiou, J. Guena, E. Penard, P. Legaud, C. Minot, J.F. Palmier, H.L. Person, and J.C. Harmand, Electron. Lett. **30**, 1690 (1994).
[3] J. Kastrup, R. Klann, H.T. Grahn, K. Ploog, L.L. Bonilla, J. Galán, M. Kindelan, M. Moscoso, and R. Merlin, Phys. Rev. B **52**, 13 761 (1995).
[4] K. Hofbeck, J. Grenzer, E. Schomburg, A.A. Ignatov, K.F. Renk, D.G. Pavel'ev, Y. Koschurinov, B. Melzer, S. Ivanov, S. Schaposchnikov, and P.S. Kop'ev, Phys. Lett. A **218**, 349 (1996).
[5] E. Schomburg, R. Scheuerer, S. Brandl, K.F. Renk, D.G. Pavel'ev, Y. Koschurinov, V. Ustinov, A. Zhukov, A. Kovsh, and P.S. Kop'ev, Electron. Lett. **35**, 1491 (1999).
[6] M. Büttiker and H. Thomas, Phys. Rev. Lett. **38**, 78 (1977).
[7] M. Patra, G. Schwarz, and E. Schöll, Phys. Rev. B **57**, 1824 (1998).
[8] R. Scheuerer, E. Schomburg, K.F. Renk, A. Wacker, and E. Schöll, Appl. Phys. Lett. **81**, 1515 (2002).
[9] L.L. Bonilla, J. Phys.: Condens. Matter **14**, R341 (2002).
[10] H. Kroemer, e-print cond-mat/0009311.
[11] E. Schöll, *Nonlinear Spatio-temporal Dynamics and Chaos in Semiconductors* (Cambridge University Press, Cambridge, 2001).
[12] Y. Zhang, J. Kastrup, R. Klann, K. Ploog, and H.T. Grahn, Phys. Rev. Lett. **77**, 3001 (1996).
[13] K.J. Luo, H.T. Grahn, K.H. Ploog, and L.L. Bonilla, Phys. Rev. Lett. **81**, 1290 (1998).
[14] O.M. Bulashenko, K.J. Luo, H.T. Grahn, K.H. Ploog, and L.L. Bonilla, Phys. Rev. B **60**, 5694 (1999).
[15] O.M. Bulashenko and L.L. Bonilla, Phys. Rev. B **52**, 7849 (1995).
[16] A. Amann, J. Schlesner, A. Wacker, and E. Schöll, Phys. Rev. B **65**, 193313 (2002).
[17] E. Schomburg, K. Hofbeck, R. Scheuerer, M. Haeussler, K.F. Renk, A.-K. Jappsen, A. Amann, A. Wacker, E. Schöll, D.G. Pavel'ev, and Y. Koschurinov, Phys. Rev. B **65**, 155320 (2002).
[18] K. Pyragas, Phys. Lett. A **170**, 421 (1992).
[19] E. Ott, C. Grebogi, and J.A. Yorke, Phys. Rev. Lett. **64**, 1196 (1990).
[20] H.G. Schuster, *Handbook of Chaos Control* (Wiley-VCH, Weinheim, 1999).
[21] S. Bielawski, D. Derozier, and P. Glorieux, Phys. Rev. E **49**, R971 (1994).
[22] T. Pierre, G. Bonhomme, and A. Atipo, Phys. Rev. Lett. **76**, 2290 (1996).
[23] K. Hall, D.J. Christini, M. Tremblay, J.J. Collins, L. Glass, and J. Billete, Phys. Rev. Lett. **78**, 4518 (1997).
[24] D.W. Sukow, M.E. Bleich, D.J. Gauthier, and J.E.S. Socolar, Chaos **7**, 560 (1997).
[25] P. Parmananda, R. Madrigal, M. Rivera, L. Nyikos, I.Z. Kiss, and V. Gáspár, Phys. Rev. E **59**, 5266 (1999).
[26] E. Benkler, M. Kreuzer, R. Neubecker, and T. Tschudi, Phys. Rev. Lett. **84**, 879 (2000).

[27] O. Lüthje, S. Wolff, and G. Pfister, Phys. Rev. Lett. **86**, 1745 (2001).
[28] H. Benner and W. Just, J. Korean Phys. Soc. **40**, 1046 (2002).
[29] C. Beta, M. Bertram, A.S. Mikhailov, H.H. Rotermund, and G. Ertl, Phys. Rev. E **67**, 046224 (2003).
[30] O. Beck, A. Amann, E. Schöll, J. Socolar, and W. Just, Phys. Rev. E **66**, 016213 (2002).
[31] A. Wacker, Phys. Rep. **357**, 1 (2002).
[32] I.R. Cantalapiedra, M.J. Bergmann, L.L. Bonilla, and S.W. Teitsworth, Phys. Rev. E **63**, 056216 (2001).
[33] M.D. Graham, U. Middya, and D. Luss, Phys. Rev. E **48**, 2917 (1993).
[34] J.E.S. Socolar, D.W. Sukow, and D.J. Gauthier, Phys. Rev. E **50**, 3245 (1994).
[35] M.E. Bleich and J.E.S. Socolar, Phys. Lett. A **210**, 87 (1996).
[36] W. Just, T. Bernard, M. Ostheimer, E. Reibold, and H. Benner, Phys. Rev. Lett. **78**, 203 (1997).
[37] H. Nakajima, Phys. Lett. A **232**, 207 (1997).
[38] G. Franceschini, S. Bose, and E. Schöll, Phys. Rev. E **60**, 5426 (1999).
[39] N. Baba, A. Amann, E. Schöll, and W. Just, Phys. Rev. Lett. **89**, 074101 (2002).
[40] W. Just, S. Popovich, A. Amann, N. Baba, and E. Schöll, Phys. Rev. E **67**, 026222 (2003).
[41] W. Just, E. Reibold, K. Kacperski, P. Fronczak, J. Holyst, and H. Benner, Phys. Rev. E **61**, 5045 (2000).